# Performance Analysis and Optimization of Hybrid MIMO Cognitive Radio Systems

Miltiades C. Filippou[1], George A. Ropokis[2], David Gesbert[3] and Tharmalingam Ratnarajah[1]

[1]Institute for Digital Communications, University of Edinburgh, Edinburgh EH9 3FG, U.K.
[2]Computer Technology Institute and Press "Diophantus", 26500, Rio-Patras, Greece
[3]Mobile Communications Department, EURECOM, 06410, Biot, France
{m.filippou, t.ratnarajah}@ed.ac.uk, ropokis@noa.gr, gesbert@eurecom.fr

***Abstract*—In this paper, the throughput performance of a hybrid Multiple-Input-Multiple-Output (MIMO) interweave/underlay Cognitive Radio (CR) system is examined on an analytical basis. Specifically, hybrid CR systems that switch between an interweave and an underlay transmission strategy, based upon spectrum sensing measurements, are investigated. For the first time the performance of such a hybrid CR system is analytically examined by deriving novel closed form approximations for the average achievable rate of the secondary system, as well as for the outage probability of the primary system. Capitalizing on the derived expressions, a new optimization problem for determining the sensing parameters, such as to maximize the average achievable rate of the secondary system, for a given outage probability of primary communication, is formulated and solved. The performance of the hybrid CR system is compared to the one achieved by the two conventional CR approaches and significant throughput gains are reported.**

***Index Terms*—cognitive radio, performance analysis, hybrid system, MIMO**

## I. Introduction

Cognitive Radio (CR) was proposed as an efficient means of dynamically allocating wireless spectrum. Till the present, two of the most important CR system categories that have been proposed are: *a*) *underlay* CR systems, where a primary system allows the simultaneous reuse of its spectral resources by a secondary system, provided that a Quality-of-Service (QoS) constraint at the Primary User (PU) is fulfilled and *b*) *interweave* CR systems, in which secondary transmitters (TXs), initially sense the spectrum, and then transmit only within time-frequency blocks, which are free of primary activity [1]. Considering the performance analysis of the aforementioned major CR approaches, substantial work has been done, especially for the calculation of the achievable average rate of the Secondary User (SU) [2]–[6].

Nonetheless, one would argue that it is meaningful to compare the throughput performance of the interweave and underlay approaches with the one achieved by a third, hybrid system, which encapsulates the advantages of both conventional CR approaches. More specifically, the interweave approach, when implemented with high quality spectrum sensing, successfully protects the PU from secondary interference. However, reliable sensing comes at the expense of increased sensing time that could lead to degraded throughput performance for the secondary system. Moreover, in the interweave approach the time intervals during which primary activity occurs remain unexploited by the CR system. On the other hand, focusing on the underlay approach, the secondary system is always in transmission mode, by applying a transmit power policy, such that the PU receives a tolerable level of interference. However, the imposed interference temperature constraint restricts secondary transmissions, even when the primary system is idle, leading to degraded throughput performance for the SU.

Based on this idea, several recent works have appeared that consider combined interweave/underlay CR approaches. In [7], a combined CR scheme, which switches between the interweave and underlay approach, based on a probabilistic criterion, is presented by exploiting results from queuing theory. However, no throughput-oriented performance analysis of this scheme is undertaken. In [8], a similar hybrid system is examined, based on a Markov chain analysis. Nevertheless, the presented results do not concern the average secondary throughput that is examined in our work. In [9], a relay-assisted hybrid CR system is proposed, along with a power allocation algorithm based on an auction game. The algorithm is based on the assumption of perfect spectrum sensing, which is rather unrealistic. In [10], a hybrid CR system is proposed for a Single-Input-Single-Output (SISO) system. Nevertheless, to the best of our knowledge, no results can be found in the literature concerning the analytical evaluation of the performance of such hybrid schemes in terms of PU outage probability and average SU system rate. More importantly, the problem of sensing optimization such as to maximize the SU average rate of such hybrid CR systems, has not been investigated.

Motivated by the above, in this paper, we study the throughput performance of hybrid interweave/underlay MIMO CR systems in an analytical manner. According to the investigated CR approach, if spectrum sensing decides upon the existence of a PU, then, the underlay CR approach is adopted, otherwise, the interweave approach is followed. Also, a maximum direct channel energy-based receive antenna selection scheme is applied. More specifically, our contributions are the following:

This work was supported by project ADEL. The Project ADEL acknowledges the financial support of the Seventh Framework Programme for Research of the European Commission under grant number: 619647. Dr. Ropokis was funded by the MIMOCORD project. The project is implemented within the framework of the Action "Supporting Postdoctoral Researchers" of the Operational Program "Education and Lifelong Learning" (Action's Beneficiary: General Secretariat for Research and Technology), and is co-financed by the European Social Fund (ESF) and the Greek State.

1) For the first time, simple closed form approximations describing the outage probability of the PU and the average achievable throughput of the SU, for the proposed hybrid CR MIMO system are derived. 2) Capitalizing on the derived results, a novel algorithm is presented for optimizing the spectrum sensing parameters of the investigated hybrid CR system. The objective of the presented optimization algorithm is the maximization of the SU throughput subject to a given QoS demand for the primary system. 3) The designed hybrid CR system is finally compared, in terms of throughput, with the two conventional CR approaches, i.e., underlay and interweave. The comparison is carried out in terms of the achievable average secondary system rate, for different targeted outage probabilities of primary communication as well as for different primary activity profiles.

The following notations are adopted in the remainder of the paper: lower case boldface letters indicate vectors and upper case boldface letters denote matrices. Superscript $(\cdot)^H$ stands for Hermitian transpose, $(\cdot)^T$ stands for matrix transpose. The identity matrix of dimension $n \times n$ is denoted by $\mathbf{I}_n$ and $\|\cdot\|$ is the Euclidean norm. $\mathbb{E}\{\cdot\}$ symbolizes the expectation operator, and $\Pr(A)$ denotes the probability of event A. For a random vector $\mathbf{x}$, $\mathbf{x} \sim \mathcal{CN}(\boldsymbol{\mu}, \boldsymbol{\Sigma})$ denotes that $\mathbf{x}$ follows a Circularly Symmetric Complex Gaussian (CSCG) distribution with mean $\boldsymbol{\mu}$ and covariance matrix $\boldsymbol{\Sigma}$. Additionally, $\mathcal{Q}(\cdot)$ stands for the complementary Gaussian distribution function [11, 4.1], whereas $E_1(\cdot)$ represents the exponential integral function, which is defined in [12, 5.1.1]. Moreover, $\Gamma(\cdot)$ denotes Gamma function defined in [12, 6.1.6], whereas $\gamma(m,x)$ and $\Gamma(m,x)$ denote the lower and upper incomplete Gamma functions, defined in [12, 6.5.2] and in [12, 6.5.3], respectively.

## II. System and channel model

The downlink of a CR system is considered that is composed of a primary TX, i.e., the Base Station, $TX\ p$, and its assigned primary receiver (RX), $RX\ p$, and a secondary TX, i.e., Base Station, $TX\ s$, with its assigned RX, $RX\ s$. It is assumed that the TXs are equipped with $M$ antennas, each, while each of the RXs is equipped with $K$ antennas. We denote the Multiple-Input-Single-Output (MISO) channel between $TX\ i$ and the $k$-th antenna of $RX\ j$, as $\mathbf{h}_{ij,k} \in \mathbb{C}^{1\times M}, \ i,j \in \{p,s\}, k = 1,\cdots,K$ and the channel between $TX\ p$ and the $m$-th antenna of $TX\ s$ as $\mathbf{h}_{00,m} \in \mathbb{C}^{1\times M}, m = 1,\cdots,M$. Rayleigh fading is assumed, i.e., it holds that $\mathbf{h}_{ij,k} \sim \mathcal{CN}(\mathbf{0}, \sigma_{ij,k}^2 \mathbf{I}_M)$ and $\mathbf{h}_{00,m} \sim \mathcal{CN}(\mathbf{0}, \sigma_{00,m}^2 \mathbf{I}_M), \ i,j \in \{p,s\}, k = 1,\cdots,K, \ m = 1,\cdots,M$. For simplicity, we assume that $\{\sigma_{ij,k}^2\}_{k=1}^K = \sigma_{ij}^2, \ i,j \in \{p,s\}$ and $\{\sigma_{00,m}^2\}_{m=1}^M = \sigma_{00}^2$.

Considering the availability of Channel State Information (CSI) at the two TXs, since we focus on a transmission scheme based on Maximal Ratio Transmission (MRT) beamforming (BF), it is assumed that $TX\ i$ has perfect knowledge of the $K \times M$ MIMO channel matrix $\mathbf{H}_{ii} = [\mathbf{h}_{ii,1}^T, \cdots, \mathbf{h}_{ii,K}^T]^T, i \in \{p,s\}$. Perfect instantaneous knowledge of the channel matrix $\mathbf{H}_{sp} = [\mathbf{h}_{sp,1}^T, \cdots, \mathbf{h}_{sp,K}^T]^T$ at both $TX\ s$ and $RX\ s$, is also considered. On the other hand, it is assumed that the MIMO interference link, $\mathbf{H}_{ps} = [\mathbf{h}_{ps,1}^T, \cdots, \mathbf{h}_{ps,K}^T]^T$, as well as the $M \times M$ channel matrix $\mathbf{H}_{00} = [\mathbf{h}_{00,1}^T, \cdots, \mathbf{h}_{00,M}^T]^T$ are statistically known to the TXs. While data transmission is based on an MRT BF policy, data reception at the RXs is based on the maximum instantaneous direct channel energy criterion that is described in the following section.

## III. Energy based receive antenna selection

We introduce random variable (RV) $X_k = \|\mathbf{h}_k\|^2, k = 1,\cdots,K$ (applicable to both the primary and the secondary direct links, only the subscript indicating the $k$-th RX antenna element is kept for simplicity). The Probability Density Function (PDF) of $X_k$ is of the form: $p_{X_k}(x) = \frac{1}{\sigma^2} p\left(\frac{x}{\sigma^2}\right)$ where $p(x) = \frac{x^{M-1}e^{-x}}{\Gamma(M)}$, with $\sigma^2 = \sigma_{pp}^2$ for the primary direct link and $\sigma^2 = \sigma_{ss}^2$ for the secondary one. The Cumulative Distribution Function (CDF) of $X_k$ is of the following form

$$P_{X_k}(x) = 1 - \frac{1}{\Gamma(M)}\Gamma\left(M, \frac{x}{\sigma^2}\right) = 1 - e^{\frac{-x}{\sigma^2}} \sum_{l=0}^{M-1} \frac{x^l}{\sigma^{2l} l!}, \quad (1)$$

where [13, 8.352.2] has been used. We now introduce RV $X = max\{X_1,\cdots,X_K\}$. Given that RVs $\{X_1,\cdots,X_K\}$ are independent, identically distributed (i.i.d.), the CDF of $X$ is readily expressed as

$$P_X(x) = Pr(X_1 \le x, \cdots, X_K \le x) = P_{X_k}(x)^K, \quad (2)$$

with $P_{X_k}(\cdot)$ given by (1). By differentiating (2), a convenient closed form expression can be derived for the PDF of $X$ for any $K$. In what follows, the hybrid interweave/underlay system, which incorporates the described receive antenna selection scheme is studied, when each RX is equipped with $K = 2$ antennas. Such a system design is in accordance with most current wireless communication standards that consider terminals equipped with two receive antennas. For such a case it is easy to show that the PDF of RV $X$ is expressed as $p_X(x) = \frac{1}{\sigma^2} p_{\max}\left(\frac{x}{\sigma^2}\right)$, where

$$p_{\max}(x) = \frac{2\left(1 - e^{-x}\sum_{m=0}^{M-1}\frac{x^m}{m!}\right)x^{M-1}e^{-x}}{\Gamma(M)}. \quad (3)$$

In the remainder, the involved MISO channels are the resulting ones, after antenna selection.

## IV. Hybrid CR model description

According to the investigated hybrid CR system, each Medium Access Control (MAC) frame, consisting of $T$ time units, is split in two subframes: 1) A subframe of $\tau$ time units, during which the secondary system is in spectrum sensing mode and 2) A subframe of $T - \tau$ time units during which data transmission takes place by the secondary system. Concerning the spectrum sensing algorithm that is applied, we assume that energy detection is used, as it is characterized by low implementation complexity and analytical expressions for its achievable performance, (i.e., false alarm and detection probabilities) [14]. Spectrum sensing takes place at one of the antennas of $TX\ s$. Finally, it is assumed that channels are fixed within the duration of a MAC frame.

In order to describe the operation of the system, we define the following events: 1) Event $\mathcal{H}_0$ that corresponds to the case that the primary system is idle, 2) event $\hat{\mathcal{H}}_0$ that corresponds to the case that no primary activity is detected, as a result of spectrum sensing. Moreover, we define the complementary of these two events, and we denote them as $\mathcal{H}_1$ and $\hat{\mathcal{H}}_1$, respectively.

### A. Spectrum sensing subframe

Following an analysis similar to the one in [6], and assuming that the transmission scheme employed by $TX\ p$ and $TX\ s$ is based on MRT BF, one can derive expressions for the false alarm probability, $\mathcal{P}_{fa}$ and the average detection probability, $\mathcal{P}_{d,av}$. Assuming the transmission of standard complex Gaussian inputs, these expressions are the following

$$\mathcal{P}_{fa} = \mathcal{Q}\left(\sqrt{N}\left(\frac{\epsilon}{N_0} - 1\right)\right), \tag{4}$$

and

$$\mathcal{P}_{d,av} = \int_0^\infty \mathcal{P}_d(\beta_{00}) f_{\beta_{00}}(\beta_{00}) d\beta_{00}, \tag{5}$$

where $\epsilon$ is the energy detection threshold, $N_0$ is the variance of the CSCG additive noise and function $\mathcal{P}_d(\beta_{00})$ is given in [6]. Also, $N = \tau f_s$ is the number of samples received by $TX\ s$ for spectrum sensing, where $f_s$ is the sampling rate for sensing. RV $\beta_{00} = |\mathbf{h}_{00}\tilde{\mathbf{h}}_{pp}^H|^2$, with $\tilde{\mathbf{h}}_{pp} = \frac{\mathbf{h}_{pp}}{\|\mathbf{h}_{pp}\|}$ is an exponentially distributed RV with parameter $\frac{1}{\sigma_{00}^2}$. The integral in (5) can be approximated either by applying the well-known Gauss-Laguerre quadrature rules [12, 25.4.45], or by deriving an approximation using Jensen's inequality [15], which is provided in [6].

### B. Data transmission subframe

By adopting MRT BF, the achievable information rate for the hybrid CR system, is given by the following expression

$$\mathcal{R}_{hyb} = \mathcal{R}_0 + \mathcal{R}_1, \tag{6}$$

where, term $\mathcal{R}_l$, $l \in \{0, 1\}$, corresponds to the achievable rate for the case that event $\hat{\mathcal{H}}_l$ occurs. In more detail, when event $\hat{\mathcal{H}}_0$ occurs, the system behaves as an interweave CR system, i.e., it transmits using a fixed transmit power $P_0$, thus, achieving a rate

$$\mathcal{R}_0 = \kappa_0 \mathcal{R}\left(\frac{P_0 \|\mathbf{h}_{ss}\|^2}{N_0}\right) + \lambda_0 \mathcal{R}\left(\frac{P_0 \|\mathbf{h}_{ss}\|^2}{N_0 + \mathcal{I}_p}\right), \tag{7}$$

with

$$\kappa_0 = \frac{(T-\tau)\mathcal{P}(\mathcal{H}_0)(1-\mathcal{P}_{fa})}{T}, \quad \lambda_0 = \frac{(T-\tau)\mathcal{P}(\mathcal{H}_1)(1-\mathcal{P}_d)}{T}, \tag{8}$$

and $\mathcal{R}(\chi) = \log_2(1+\chi)$. In (7), $\mathcal{I}_p$ stands for the quantity $\mathcal{I}_p = P_p|\mathbf{h}_{ps}\tilde{\mathbf{h}}_{pp}^H|^2$, where $P_p$ denotes the fixed instantaneous power emitted by $TX\ p$.

On the other hand, when the system chooses to apply the underlay CR approach, i.e., when event $\hat{\mathcal{H}}_1$ occurs, a power policy based on knowledge of the instantaneous interference caused by secondary transmission to primary communication is employed. In more detail, following the approach presented in [5] [6], the transmission power policy is of the form:

$$P_1 = \min\left\{\frac{\mathcal{I}}{|\mathbf{h}_{sp}\tilde{\mathbf{h}}_{ss}^H|^2}, P_s\right\}, \tag{9}$$

where $\mathcal{I}$ stands for the maximum tolerated interference power at the PU and $P_s$ for the maximum available instantaneous power at $TXs$. In our analysis, we assume that $P_s = P_0$. When such a transmission policy is applied, the achievable rate is

$$\mathcal{R}_1 = \kappa_1 \mathcal{R}\left(\frac{P_1 \|\mathbf{h}_{ss}\|^2}{N_0}\right) + \lambda_1 \mathcal{R}\left(\frac{P_1 \|\mathbf{h}_{ss}\|^2}{N_0 + \mathcal{I}_p}\right), \tag{10}$$

$$\text{with} \quad \kappa_1 = \frac{(T-\tau)\mathcal{P}(\mathcal{H}_0)\mathcal{P}_{fa}}{T}, \quad \lambda_1 = \frac{(T-\tau)\mathcal{P}(\mathcal{H}_1)\mathcal{P}_d}{T}. \tag{11}$$

In the following section, a closed form approximation for the outage probability at the PU, when the investigated hybrid CR system is used, is derived.

## V. Outage probability of primary communication

The primary system experiences an outage event, when given that it is active, the Signal-to-Interference-plus-Noise Ratio (SINR) of the PU falls below a target value, $\gamma_0$. In the following proposition, a closed form approximation for the outage probability of the PU is provided.

*Proposition* 1. The outage probability of primary communication for a MIMO hybrid CR system, with $K = 2$ antennas at each RX, and energy-based antenna selection at RX, is given by the following expression

$$\mathcal{P}_{out}^{hyb} = \mathcal{P}_{out,0} + \mathcal{P}_{out,1}, \tag{12}$$

$$\text{where,} \quad \mathcal{P}_{out,0} = (1-\mathcal{P}_{d,av}) \underbrace{\Pr\left(\frac{P_p\|\mathbf{h}_{pp}\|^2}{N_0 + P_0|\mathbf{h}_{sp}\tilde{\mathbf{h}}_{ss}^H|^2} < \gamma_0\right)}_{\mathcal{P}_1}, \tag{13}$$

and $\tilde{\mathbf{h}}_{ss} = \frac{\mathbf{h}_{ss}}{\|\mathbf{h}_{ss}\|}$. Probability $\mathcal{P}_1$ is given by $\mathcal{P}_1 = \frac{2}{\Gamma(M)\sigma_2^2}(Q_1 - Q_2)$, where $\sigma_2^2 = \gamma_0 P_0 \sigma_{sp}^2$. Terms $Q_1$ and $Q_2$ are given by

$$Q_1 = \Gamma(M)\left(\sigma_2^2 - e^{\frac{\gamma_0 N_0}{\sigma_2^2}} \sum_{m=0}^{M-1} \frac{\Gamma\left(m+1, \gamma_0 N_0\left(\frac{\sigma_1^2+\sigma_2^2}{\sigma_1^2\sigma_2^2}\right)\right)}{m!\sigma_1^{2m}\left(\frac{\sigma_1^2+\sigma_2^2}{\sigma_1^2\sigma_2^2}\right)^{m+1}}\right), \tag{14}$$

and

$$Q_2 = \sum_{m=0}^{M-1} \frac{\Gamma(m+M)}{m!2^{m+M}}\left(\sigma_2^2 - e^{\frac{\gamma_0 N_0}{\sigma_2^2}} \times \sum_{n=0}^{m+M-1} \frac{2^n\Gamma\left(n+1, \gamma_0 N_0\left(\frac{\sigma_1^2+2\sigma_2^2}{\sigma_1^2\sigma_2^2}\right)\right)}{n!\sigma_1^{2n}\left(\frac{\sigma_1^2+2\sigma_2^2}{\sigma_1^2\sigma_2^2}\right)^{n+1}}\right), \tag{15}$$

where $\sigma_1^2 = P_p \sigma_{pp}^2$. Regarding probability $\mathcal{P}_{out,1}$, this is given by

$$\mathcal{P}_{out,1} = \mathcal{P}_{d,av}\Bigg( \Pr(\mathcal{E}) \Pr\left( \frac{P_p \|\mathbf{h}_{pp}\|^2}{N_0 + \mathcal{I}} < \gamma_0 \right) + \Pr\left( \mathcal{E}', \frac{P_p \|\mathbf{h}_{pp}\|^2}{N_0 + P_0 |\mathbf{h}_{sp} \tilde{\mathbf{h}}_{ss}^H|^2} < \gamma_0 \right) \Bigg) = \mathcal{P}_{d,av} \mathcal{P}_2, \tag{16}$$

where $\mathcal{E}$ denotes the event $\frac{\mathcal{I}}{|\mathbf{h}_{sp} \tilde{\mathbf{h}}_{ss}^H|^2} \leq P_0$ and $\mathcal{E}'$ its complement. Moreover, it is easy to show that

$$\Pr(\mathcal{E}) = e^{-\frac{\mathcal{I}}{P_0 \sigma_{sp}^2}}. \tag{17}$$

The two remaining probabilities that are involved in (16) are given as

$$\Pr\left( \frac{P_p \|\mathbf{h}_{pp}\|^2}{N_0 + \mathcal{I}} < \gamma_0 \right) = \frac{2}{\Gamma(M)} \Bigg( \gamma\left( M, \frac{\gamma_0 (N_0 + \mathcal{I})}{\sigma_1^2} \right) - \sum_{m=0}^{M-1} \frac{1}{m! 2^{m+M}} \gamma\left( m + M, \frac{2\gamma_0 (N_0 + \mathcal{I})}{\sigma_1^2} \right) \Bigg), \tag{18}$$

and

$$\begin{aligned} &\Pr\left( \mathcal{E}', \frac{P_p \|\mathbf{h}_{pp}\|^2}{N_0 + P_0 |\mathbf{h}_{sp} \tilde{\mathbf{h}}_{ss}^H|^2} < \gamma_0 \right) = \frac{2\gamma_0 P_0}{\Gamma(M) \sigma_1^{2M} \sigma_2^2} \times \\ &\Bigg( \Gamma(M) \sigma_1^{2M} \left( \frac{\sigma_2^2}{\gamma_0 P_0} (1 - e^{-\frac{\gamma_0 \mathcal{I}}{\sigma_2^2}}) - \sum_{m=0}^{M-1} \frac{e^{\frac{-\gamma_0 N_0}{\sigma_1^2}}}{m! \sigma_1^{2m}} A\left( \frac{\sigma_1^2 + \sigma_2^2}{\sigma_1^2 \sigma_2^2}, m \right) \right) \\ &- \sum_{m=0}^{M-1} \frac{\sigma_1^{2M}}{m! 2^{m+M}} \Gamma(m+M) \Bigg( \frac{\sigma_2^2}{\gamma_0 P_0} (1 - e^{-\frac{\gamma_0 \mathcal{I}}{\sigma_2^2}}) \\ &- \sum_{n=0}^{m+M-1} \frac{2^n e^{-\frac{2\gamma_0 N_0}{\sigma_1^2}}}{n! \sigma_1^{2n}} A\left( \frac{\sigma_1^2 + 2\sigma_2^2}{\sigma_1^2 \sigma_2^2}, n \right) \Bigg) \Bigg), \end{aligned} \tag{19}$$

where

$$A(\tilde{\alpha}, i) = \frac{e^{\gamma_0 N_0 \tilde{\alpha}} \left( \Gamma\left( i+1, \gamma_0 N_0 \tilde{\alpha} \right) - \Gamma\left( i+1, \gamma_0 (N_0 + \mathcal{I}) \tilde{\alpha} \right) \right)}{\gamma_0 P_0 \tilde{\alpha}^{i+1}}. \tag{20}$$

*Proof.* The outage probability of primary communication, for the examined hybrid CR system, is given by the following generic expression

$$\mathcal{P}_{out}^{hyb} = \underbrace{Pr\left( SINR_{p,0} < \gamma_0 | \hat{\mathcal{H}}_0, \mathcal{H}_1 \right)}_{\mathcal{P}_{out,0}} + \underbrace{Pr\left( SINR_{p,1} < \gamma_0 | \hat{\mathcal{H}}_1, \mathcal{H}_1 \right)}_{\mathcal{P}_{out,1}}, \tag{21}$$

where

$$SINR_{p,l} = \frac{P_p \|\mathbf{h}_{pp}\|^2}{N_0 + P_l |\mathbf{h}_{sp} \tilde{\mathbf{h}}_{ss}^H|^2}, \tag{22}$$

stands for the primary communication SINR given that the joint event $\hat{\mathcal{H}}_l \cap \mathcal{H}_1$, $l \in \{0, 1\}$ has occurred. Closed form approximations for the terms of (21) can be derived by exploiting the known distributions of RVs $\|\mathbf{h}_{pp}\|^2 = \max\{\|\mathbf{h}_{pp,1}\|^2, \|\mathbf{h}_{pp,2}\|^2\}$ and $|\mathbf{h}_{sp} \tilde{\mathbf{h}}_{ss}^H|^2$ as well as [13, 3.351.1], [13, 3.351.2] and [13, 8.352.6]. The PDF of the first RV is given by employing (3) , while the second RV is exponentially distributed with parameter $\frac{1}{\sigma_{sp}^2}$. A more detailed proof for the derivation of the involved terms can be found in [6]. □

In the following, an approximate expression of the achievable average rate at the SU, is derived.

## VI. Ergodic rate of secondary communication

The achievable average rate at the SU, is given by the following expression

$$\mathbb{E}\{\mathcal{R}_{hyb}\} = \mathbb{E}\{\mathcal{R}_0\} + \mathbb{E}\{\mathcal{R}_1\}. \tag{23}$$

In the following subsections, the procedure for calculating the two expectations in the right hand side of (23) is presented. To facilitate the presentation of the resulting expressions, we define the functions

$$\mathcal{G}(\alpha, L) = \sum_{\mu=0}^{L-1} \frac{\Gamma(L)}{\Gamma(L-\mu)} \Bigg( \frac{(-1)^{L-\mu-3}}{\alpha^{L-\mu-1}} e^{\frac{1}{\alpha}} E_1\left( \frac{1}{\alpha} \right) + \sum_{k=1}^{L-\mu-1} \Gamma(k) \left( -\frac{1}{\alpha} \right)^{L-\mu-k-1} \Bigg), \tag{24}$$

$$\text{and} \quad \mathcal{F}(\alpha, \beta, L) = \mathcal{G}(\alpha, L) + \ln(\beta) \Gamma(L). \tag{25}$$

### A. Computation of $\mathbb{E}\{\mathcal{R}_0\}$

Since antenna selection is applied at the SU, the PDF of $\|\mathbf{h}_{ss}\|^2$ is given by (3). Also, RV $|\mathbf{h}_{ps} \tilde{\mathbf{h}}_{pp}^H|^2$ is exponentially distributed with parameter equal to $\frac{1}{\sigma_{ps}^2}$. Hence, focusing initially on the calculation of $\mathbb{E}\{\mathcal{R}_0\}$, it follows that

$$\mathbb{E}\left\{ \mathcal{R}\left( \frac{P_0 \|\mathbf{h}_{ss}\|^2}{N_0} \right) \right\} = \frac{2\left( \mathcal{T}_1\left( \frac{P_0 \sigma_{ss}^2}{N_0} \right) - \mathcal{T}_2\left( \frac{P_0 \sigma_{ss}^2}{N_0} \right) \right)}{\ln(2) \Gamma(M)}, \tag{26}$$

where by applying [13, 4.337.5], $\mathcal{T}_1(\cdot)$ and $\mathcal{T}_2(\cdot)$, are expressed as

$$\mathcal{T}_1(\alpha) = \mathcal{G}(\alpha, M), \text{and} \quad \mathcal{T}_2(\alpha) = \sum_{m=0}^{M-1} \frac{1}{m! 2^{m+M}} \mathcal{G}\left( \frac{\alpha}{2}, M+m \right). \tag{27}$$

Moreover, it is easy to show that

$$\mathbb{E}\left\{ \mathcal{R}\left( \frac{P_0 \|\mathbf{h}_{ss}\|^2}{N_0 + \mathcal{I}_p} \right) \right\} = \frac{1}{\ln(2)} (\mathcal{J}_1 - \mathcal{J}_2). \tag{28}$$

After some algebraic manipulations exploiting [13, 4.337.1] and [13, 3.351.3], quantity $\mathcal{J}_1$ is found to be

$$\mathcal{J}_1 = \frac{2}{\Gamma(M)} \Bigg( \mathcal{F}\left( \frac{P_0 \sigma_{ss}^2}{N_0}, N_0, M \right) - \sum_{m=0}^{M-1} \frac{(\mathcal{J}_{1,1}(m) + \mathcal{J}_{1,2}(m))}{(P_0 \sigma_{ss}^2)^{m+M} m!} + \int_0^\infty e^{-u} u^{M-1} e^{\frac{N_0 + P_0 \sigma_{ss}^2 u}{P_p \sigma_{ps}^2}} E_1\left( \frac{N_0 + P_0 \sigma_{ss}^2 u}{P_p \sigma_{ps}^2} \right) du \Bigg), \tag{29}$$

where terms $\mathcal{J}_{1,1}(m)$ and $\mathcal{J}_{1,2}(m)$ are given by the following expressions

$$\mathcal{J}_{1,1}(m) = \left( \frac{P_0 \sigma_{ss}^2}{2} \right)^{m+M} \mathcal{F}\left( \frac{P_0 \sigma_{ss}^2}{2N_0}, N_0, m+M \right), \tag{30}$$

where [13, 4.337.5] has been used, and

$$\mathcal{J}_{1,2}(m) = e^{\frac{N_0}{P_p\sigma_{ps}^2}}\delta^{m+M}\int_0^\infty e^{-v}v^{m+M-1}E_1\left(\frac{N_0+\delta v}{P_p\sigma_{ps}^2}\right)dv, \quad (31)$$

where $\delta = \frac{P_0 P_p \sigma_{ss}^2\sigma_{ps}^2}{2P_p\sigma_{ps}^2 - P_0\sigma_{ss}^2}$. It should be noted that the integrals appearing in (29) and (31) can be approximated by applying the Gauss-Laguerre quadrature rules.

Finally, the derivation of term $\mathcal{J}_2$, by applying [13, 4.337.1], gives

$$\mathcal{J}_2 = \ln(N_0) + e^{\frac{N_0}{P_p\sigma_{ps}^2}}E_1\left(\frac{N_0}{P_p\sigma_{ps}^2}\right). \quad (32)$$

Hence $\mathbb{E}\{\mathcal{R}_0\}$ is expressed as

$$\mathbb{E}\{\mathcal{R}_0\} = \frac{2\kappa_0}{\ln(2)\Gamma(M)}\left(\mathcal{T}_1\left(\frac{P_0\sigma_{ss}^2}{N_0}\right) - \mathcal{T}_2\left(\frac{P_0\sigma_{ss}^2}{N_0}\right)\right) + \frac{\lambda_0}{\ln(2)}(\mathcal{J}_1 - \mathcal{J}_2). \quad (33)$$

In what follows, we derive an expression for the achievable average SU rate, when the hybrid CR system operates according to the underlay CR approach.

## B. Computation of $\mathbb{E}\{\mathcal{R}_1\}$

Taking into consideration the truncated power policy, which is described in (9), the achievable rate for this approach is split in two terms, i.e., it is written in the form

$$\mathbb{E}\{\mathcal{R}_1\} = \kappa_1\mathcal{B}_0 + \lambda_1\mathcal{B}_1, \quad (34)$$

where each term in the right hand side of (34) corresponds to a different event, i.e., events $\mathcal{H}_0$ and $\mathcal{H}_1$ respectively. Regarding $\mathcal{B}_0$, this is given as

$$\mathcal{B}_0 = \underbrace{\mathbb{E}_{\|\mathbf{h}_{ss}\|^2}\left\{\int_{\frac{\mathcal{I}}{P_0}}^\infty \mathcal{R}\left(\frac{\mathcal{I}\|\mathbf{h}_{ss}\|^2}{N_0 z}\right)p_z(z)\,dz\right\}}_{\mathbb{E}\{\mathcal{C}_1\}} + \Pr(\mathcal{E}')\underbrace{\mathbb{E}\left\{\mathcal{R}\left(\frac{P_0\|\mathbf{h}_{ss}\|^2}{N_0}\right)\right\}}_{\mathbb{E}\{\mathcal{C}_2\}}, \quad (35)$$

where we have introduced the auxiliary chi-squared distributed RV $z = |\mathbf{h}_{sp}\tilde{\mathbf{h}}_{ss}^H|^2$. For the computation of $\mathbb{E}\{\mathcal{C}_1\}$, we have

$$\mathbb{E}\{\mathcal{C}_1\} = \frac{1}{\ln(2)}(\mathcal{K}_1 - \mathcal{K}_2), \quad (36)$$

where $\mathcal{K}_1$, is given by [13, 3.352.2]

$$\mathcal{K}_1 = \frac{2e^{-\frac{\mathcal{I}}{P_s\sigma_{sp}^2}}}{\Gamma(M)}(\mathcal{K}_{1,1} - \mathcal{K}_{1,2}) + \mathcal{K}_{1,3}, \quad (37)$$

where, by exploiting [13, 3.351.3] and [13, 4.337.5]

$$\mathcal{K}_{1,1} = \mathcal{F}\left(\frac{P_0\sigma_{ss}^2}{N_0}, \frac{N_0\mathcal{I}}{P_0}, M\right), \quad (38)$$

$$\mathcal{K}_{1,2} = \sum_{m=0}^{M-1}\frac{\mathcal{F}\left(\frac{P_0\sigma_{ss}^2}{2N_0}, \frac{N_0\mathcal{I}}{P_0}, m+M\right)}{m!2^{m+M}}, \quad (39)$$

and

$$\mathcal{K}_{1,3} = \int_0^\infty p_{\max}(u)\,e^{\frac{\mathcal{I}\sigma_{ss}^2 u}{N_0\sigma_{sp}^2}}E_1\left(\frac{\mathcal{I}}{P_0\sigma_{sp}^2} + \frac{\mathcal{I}\sigma_{ss}^2 u}{N_0\sigma_{sp}^2}\right)du, \quad (40)$$

which can be approximated by the use of Gauss-Laguerre quadratic rules. Term $\mathcal{K}_2$ on the other hand is of the following form

$$\mathcal{K}_2 = \ln\left(\frac{N_0\mathcal{I}}{P_0}\right)e^{-\frac{\mathcal{I}}{P_0\sigma_{sp}^2}} + E_1\left(\frac{\mathcal{I}}{P_0\sigma_{sp}^2}\right). \quad (41)$$

For the computation of $\mathbb{E}\{\mathcal{C}_2\}$, it is easy to see that it holds that

$$\mathbb{E}\{\mathcal{C}_2\} = \frac{2\left(\mathcal{T}_1\left(\frac{P_0\sigma_{ss}^2}{N_0}\right) - \mathcal{T}_2\left(\frac{P_0\sigma_{ss}^2}{N_0}\right)\right)}{\ln(2)\Gamma(M)}. \quad (42)$$

Regarding term $\mathcal{B}_1$, this is expressed as

$$\mathcal{B}_1 = \mathbb{E}_{\|\mathbf{h}_{ss}\|^2,\mathcal{I}_p}\left\{\int_{\frac{\mathcal{I}}{P_0}}^\infty \mathcal{R}\left(\frac{\mathcal{I}\|\mathbf{h}_{ss}\|^2}{z(N_0+\mathcal{I}_p)}\right)p_z(z)dz\right\} + \Pr(\mathcal{E}')\,\mathbb{E}\left\{\mathcal{R}\left(\frac{P_0\|\mathbf{h}_{ss}\|^2}{N_0+\mathcal{I}_p}\right)\right\}. \quad (43)$$

For the first term in the right hand side of (43), we have that

$$\mathbb{E}_{\|\mathbf{h}_{ss}\|^2,\mathcal{I}_p}\left\{\int_{\frac{\mathcal{I}}{P_0}}^\infty \mathcal{R}\left(\frac{\mathcal{I}\|\mathbf{h}_{ss}\|^2}{z(N_0+\mathcal{I}_p)}\right)p_z(z)dz\right\} = \frac{(\mathcal{L}_1 - \mathcal{L}_2)}{\ln(2)}, \quad (44)$$

where, using [13, 3.352.2], it can be shown that

$$\mathcal{L}_1 = \frac{2e^{-\frac{\mathcal{I}}{P_0\sigma_{sp}^2}}}{\Gamma(M)}(\mathcal{L}_{1,1} - \mathcal{L}_{1,2}) + \mathcal{L}_{1,3} + \mathcal{L}_{1,4}. \quad (45)$$

The derivation of the first term of (45), after applying [13, 3.351.3], gives

$$\mathcal{L}_{1,1} = \mathcal{K}_{1,1}, \qquad \mathcal{L}_{1,2} = \mathcal{K}_{1,2}, \quad (46)$$

where $\mathcal{K}_{1,1}$ and $\mathcal{K}_{1,2}$ were derived in (38) and (39), respectively.

Also, for the second and third term of (45), one obtains

$$\mathcal{L}_{1,3} = \int_0^\infty p_{\max}(u)\,e^{\left(\frac{P_0\sigma_{ss}^2 u}{P_p\sigma_{ps}^2} + \frac{N_0}{P_p\sigma_{ps}^2}\right)}E_1\left(\frac{P_0\sigma_{ss}^2 u}{P_p\sigma_{ps}^2} + \frac{N_0}{P_p\sigma_{ps}^2}\right)du, \quad (47)$$

and

$$\mathcal{L}_{1,4} = \int_0^\infty\int_0^\infty e^{-w}p_{\max}(u) \times e^{\frac{\mathcal{I}\sigma_{ss}^2 u}{\sigma_{sp}^2(N_0+P_p\sigma_{ps}^2 w)}}E_1\left(\frac{\mathcal{I}\sigma_{ss}^2 u}{\sigma_{sp}^2(N_0+P_p\sigma_{ps}^2 w)} + \frac{\mathcal{I}}{P_0\sigma_{sp}^2}\right)dwdu. \quad (48)$$

The values of the integrals appearing in the last two expressions can be approximated by applying the Gauss-Laguerre quadrature rules for a single and a two-dimensional case, respectively [12, 25.4.45]. Moreover, term $\mathcal{L}_2$, by exploiting [13, 3.352.2], is written as

$$\mathcal{L}_2 = e^{-\frac{\mathcal{I}}{P_0\sigma_{sp}^2}}\left(\ln\left(\frac{N_0\mathcal{I}}{P_0}\right) + e^{\frac{N_0}{P_p\sigma_{ps}^2}}E_1\left(\frac{N_0}{P_p\sigma_{ps}^2}\right)\right) + E_1\left(\frac{\mathcal{I}}{P_0\sigma_{sp}^2}\right). \quad (49)$$

Finally, the expectation appearing in the second term of the right hand side of (43), is given by (28).

In the following section, an optimization problem is formulated in order to optimally select sensing parameters i.e., $\tau$ and $\epsilon$ such as to maximize the average rate of the SU for a given outage probability of the PU.

## VII. Optimizing the Spectrum Sensing Parameters

The average SU rate-optimal values of the sensing time, $\tau^*$ and the energy detection threshold, $\epsilon^*$, for a target PU outage probability, $\mathcal{P}_t$, can be found by solving the following problem

$$\begin{aligned}(\epsilon^*, \tau^*) &= \arg\max_{\epsilon,\tau} \ \ \mathbb{E}\{\mathcal{R}_{hyb}\} \\ s.t. \ \ \mathcal{P}_{out}^{hyb} &= \mathcal{P}_t, \quad 0 < \tau \leq T, \quad \epsilon \geq 0,\end{aligned} \tag{50}$$

where $\mathcal{P}_{out}^{hyb}$ is given by Proposition 1. The equality constraint can be equivalently written as

$$\mathcal{P}_{d,av}(\tau, \epsilon) = \frac{\mathcal{P}_t - \mathcal{P}_1}{\mathcal{P}_2 - \mathcal{P}_1}, \tag{51}$$

where, probabilities $\mathcal{P}_1$ and $\mathcal{P}_2$ are given in Proposition 1 and $\mathcal{P}_2 = \mathcal{P}_2(\mathcal{I})$. Since our ultimate intention is to compare the throughput of the hybrid CR system with the one achieved by the two conventional CR approaches, given that a targeted PU outage probability, $\mathcal{P}_t$ leads to a certain threshold, $\mathcal{I}$, for the conventional underlay approach, the same value of $\mathcal{I}$ will be used in (51). This value can be found by applying the bisection algorithm for the conventional underlay CR approach (which incorporates no sensing), where $\kappa_1 = \mathcal{P}(\mathcal{H}_0)$ and $\lambda_1 = \mathcal{P}(\mathcal{H}_1)$.

In order to find the sensing parameters, $\tau^*$ and $\epsilon^*$, which maximize the average SU rate, an exhaustive search over the number of samples, $N$, can be applied by searching the discrete number set $[1, Tf_s]$, and an appropriate value for threshold $\epsilon$ can be found with bisection in order to fulfill the PU outage probability constraint. Alternatively, one can apply the Jensen-based approximation of $\mathcal{P}_{d,av}$ given in [6, 6]. In this case, the PU outage probability constraint leads to an expression $\epsilon = f(\tau)$, where $f(x) = m_s\left(\frac{\zeta}{\sqrt{xf_s}} + 1\right)$, with $m_s = P_p\sigma_{00}^2 + N_0$ and $\zeta = Q^{-1}\left(\frac{\mathcal{P}_t - \mathcal{P}_1}{\mathcal{P}_2 - \mathcal{P}_1}\right)$. By applying the second derivative criterion for the objective function $\mathbb{E}\{\mathcal{R}_{hyb}(\tau, \epsilon(\tau))\}$, it can be proved that the latter is a concave function of $\tau$ for $\tau \in (0, T]$, when $P_s = P_0$. As a result, any convex optimization algorithm can be applied in order to find $\tau^*$ and thus $\epsilon^*$.

*Remark*: It can be validated by simulation that the two approximations of $\mathcal{P}_{d,av}$, achieve similar average SU rates for the optimal values of the sensing parameters, when either the exhaustive search algorithm (for the Laguerre-based approximation) or a convex optimization method (for the Jensen-based approximation), are applied.

## VIII. Numerical Evaluation

Extensive Monte Carlo (MC) simulations have been performed with the aim of cross-validating the correctness of the theoretical expressions derived. More specifically, 5000 MAC frames have been simulated. According to the simulation scenario, each TX is equipped with $M = 4$ antennas, while each RX is equipped with $K = 2$ antennas. The variances of the involved channel links are: $\sigma_{pp}^2 = \sigma_{ss}^2 = 10$dB, $\sigma_{sp}^2 = 9$dB, $\sigma_{ps}^2 = 8.45$dB and $\sigma_{00}^2 = 7.8$dB. Additionally, we set $f_s = 6$MHz, $T = 100$ms, while unit variance noise is considered. The SINR threshold below which an outage event at the PU is declared, is $\gamma_0 = 9$dB.

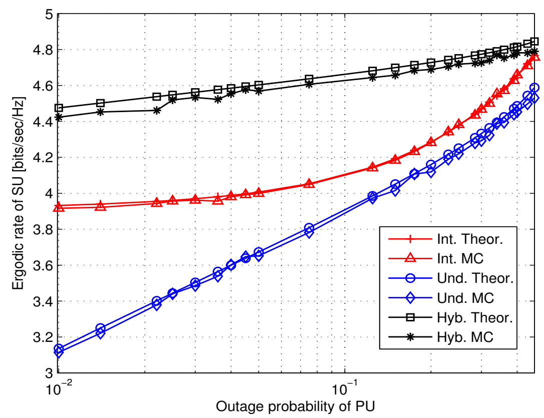


Fig. 1. Ergodic SU rate vs. PU outage probability, $\mathcal{P}_t$, $\mathcal{P}(\mathcal{H}_1) = 0.3$.

In Fig. 1, the achievable average SU rate is depicted as a function of the outage probability of primary communication, $\mathcal{P}_t$, for a system setup characterized by relatively low primary activity (i.e., $\mathcal{P}(\mathcal{H}_1) = 0.3$). Both MC and theoretical curves are illustrated with respect to the investigated hybrid CR system as well as for the interweave and underlay CR approaches. Considering the two conventional CR approaches, the SU rate-optimal design parameters are found, by solving problems equivalent to (50) that are presented in detail in [6]. One can observe that the MC-based curves closely converge to the ones corresponding to the derived approximate expressions for the average SU rate. This confirms the validity of the derived expressions. Secondly, it is evident that the hybrid CR system outperforms the two conventional CR approaches for the whole examined PU outage probability interval. This happens because, in contrast with the underlay CR approach, where only a fraction of the total power of $TX\ s$ is constantly emitted regardless of the activity profile of the primary system, under the hybrid CR system, there are times where, as a result of sensing decisions upon the absence of the PU, full transmit power is emitted by $TX\ s$. On the other hand, unlike the interweave CR approach, where, when primary activity is detected by sensing, $TX\ s$ becomes silent during the data transmission subframe, according to the hybrid CR system, secondary transmission is still carried out by switching to the underlay CR mode. This allows for better exploitation of the shared frequency resources.

In Fig. 2 the same curves are illustrated, this time for a system scenario, according to which, the primary network is busy for 70% of the time. In this case, the hybrid CR system still outperforms the two conventional CR approaches, however, the performance of the underlay CR system now overcomes the one achieved by the interweave CR system. This is due to the fact that high primary activity profiles result in reducing the time slots during which the frequency resources are free for use by the interweave CR system. Thus, the achievable throughput of the interweave CR system is reduced. It should be also noted that for both system setups, all curves are increasing as a function of $\mathcal{P}_t$. This occurs, because as the targeted PU outage probability becomes higher, the equivalent maximum tolerated interference at the PU also increases, hence, for all examined approaches, $TX\ s$ allocates the available resources primarily with the aim of maximizing the SU rate. Finally, fixing a value for $\mathcal{P}_t$, the average SU rate for all approaches will be lower for highly active primary systems. This can be explained by the fact that when $\mathcal{P}(\mathcal{H}_1)$ becomes closer to one, more interference by primary transmissions is experienced by $RX\ s$, on average.

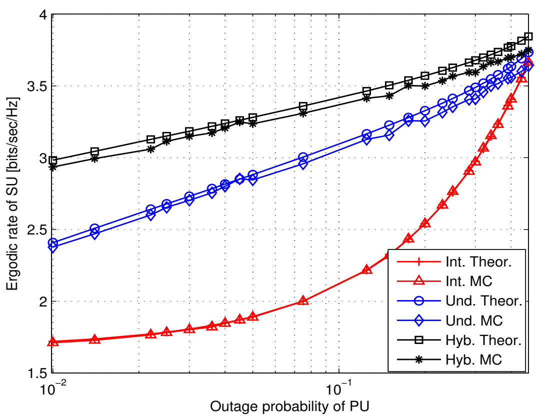


Fig. 2. Ergodic SU rate vs. PU outage probability, $\mathcal{P}_t$, $\mathcal{P}(\mathcal{H}_1) = 0.7$.

## IX. Conclusions

The performance analysis of a hybrid interweave/underlay MIMO CR system is analytically investigated in this paper, along with the optimization of the sensing parameters, aiming at maximizing its average SU rate. Expressions for the PU outage probability and the average SU rate are derived and the SU throughput performance of the hybrid system is compared with the one achieved by the interweave (with SU rate-optimal spectrum sensing) and underlay approaches. It is shown that the hybrid system outperforms the conventional ones for the investigated primary activity profiles. Interesting extensions can be made in terms of investigating the existence of multiple primary and secondary terminals, where the former will conduct collaborative spectrum sensing.

## References

[1] E. Biglieri, A. J. Goldsmith, L. J. Greenstein, N. Mandayam, and H. V. Poor, *Principles of Cognitive Radio*. Cambridge University Press, 2012.

[2] H. A. Suraweera, P. J. Smith, and M. Shafi, “Capacity limits and performance analysis of cognitive radio with imperfect channel knowledge,” *IEEE Transactions on Vehicular Technology*, vol. 59, no. 4, pp. 1811–1822, 2010.

[3] X. Kang, Y.-C. Liang, A. Nallanathan, H. Garg, and R. Zhang, “Optimal power allocation for fading channels in cognitive radio networks: Ergodic capacity and outage capacity,” *IEEE Transactions on Wireless Communications*, vol. 8, no. 2, pp. 940–950, Feb. 2009.

[4] K. Tourki, F. Khan, K. Qaraqe, H.-C. Yang, and M.-S. Alouini, “Exact performance analysis of MIMO cognitive radio systems using transmit antenna selection,” *IEEE Journal on Selected Areas in Communications*, vol. 32, no. 3, pp. 425–438, Mar. 2014.

[5] M. Filippou, D. Gesbert, and G. Ropokis, “Underlay versus interweaved cognitive radio networks: A performance comparison study,” in *2014 9th International Conference on Cognitive Radio Oriented Wireless Networks and Communications (CROWNCOM)*, Jun. 2014, pp. 226–231.

[6] ——, “A comparative performance analysis of interweave and underlay multi-antenna cognitive radio networks,” *IEEE Transactions on Wireless Communications*, 2015, to appear.

[7] J. Oh and W. Choi, “A hybrid cognitive radio system: A combination of underlay and overlay approaches,” in *2010 IEEE 72nd Vehicular Technology Conference Fall (VTC 2010-Fall)*, Sep. 2010, pp. 1–5.

[8] S. Senthuran, A. Anpalagan, and O. Das, “Throughput analysis of opportunistic access strategies in hybrid underlay-overlay cognitive radio networks,” *IEEE Transactions on Wireless Communications*, vol. 11, no. 6, pp. 2024–2035, Jun. 2012.

[9] J. Zou, H. Xiong, D. Wang, and C. W. Chen, “Optimal power allocation for hybrid overlay/underlay spectrum sharing in multiband cognitive radio networks,” *IEEE Transactions on Vehicular Technology*, vol. 62, no. 4, pp. 1827–1837, May 2013.

[10] H. Song, J.-P. Hong, and W. Choi, “On the optimal switching probability for a hybrid cognitive radio system,” *IEEE Transactions on Wireless Communications*, vol. 12, no. 4, pp. 1594–1605, Apr. 2013.

[11] M. K. Simon and M.-S. Alouini, *Digital communication over fading channels*. John Wiley & Sons, 2005, vol. 95.

[12] M. Abramowitz and I. A. Stegun, *Handbook of mathematical functions*. Dover publications, 1965.

[13] I. S. Gradshteyn and I. M. Ryzhik, *Table of integrals, series, and products*, 7th ed. Elsevier/Academic Press, Amsterdam, 2007.

[14] Y.-C. Liang, Y. Zeng, E. Peh, and A. T. Hoang, “Sensing-throughput tradeoff for cognitive radio networks,” *IEEE Transactions on Wireless Communications*, vol. 7, no. 4, pp. 1326–1337, Apr. 2008.

[15] T. M. Cover and J. A. Thomas, *Elements of information theory*. John Wiley & Sons, 2012.